

Reduced Ionic Diffusion by the Dynamic Electron-Ion Collisions in Warm Dense Hydrogen

Yunpeng Yao,¹ Qiyu Zeng,¹ Ke Chen,¹ Dongdong Kang,¹ Yong Hou,¹ Qian Ma,¹ and Jiayu Dai^{1, a)}
*Department of Physics, National University of Defense Technology, Changsha, Hunan 410073,
 P. R. China*

(Dated: 5 January 2021)

The dynamic electron-ion collisions play an important role in determining the static and transport properties of warm dense matter (WDM). Electron force field (eFF) method is applied to study the ionic transport properties of warm dense hydrogen. Compared with the results from quantum molecular dynamics and orbital-free molecular dynamics, the ionic diffusions are largely reduced by involving the dynamic collisions of electrons and ions. This physics is verified by the quantum Langevin molecular dynamics (QLMD) simulations, which includes electron-ion collisions induced friction (EI-CIF) into the dynamic equation of ions. Based on these new results, we proposed a model including the correction of collisions induced friction of the ionic diffusion. The CIF model has been verified to be valid at a wide range of density and temperature. We also compare the results with the Yukawa one component plasma (YOCP) model and Effective OCP (EOCP) model. We proposed to calculate the self-diffusion coefficients using the EOCP model modified by the CIF model to introduce the dynamic electron-ion collisions effect.

I. INTRODUCTION

Warm dense matter (WDM) is an intermediate state bridges the condensed matter and ideal plasma¹. The transport properties of WDM, such as diffusion, viscosity, thermal conduction, and temperature relaxation, etc.²⁻⁶, play important roles in the field of astrophysics and inertial confinement fusion⁷⁻¹¹ (ICF). For WDM, the ionic coupling parameter $\Gamma = Z_i^2 e^2 / (r_i k_B T)$ is larger than 1, and the electron degeneracy parameter $\Theta = T/T_F$ is less than 1. That requires us to consider both strong coupling between ions and the partial ionization and partial degeneration of electrons when studying the unique state. There has not been a mature theory that is good enough to describe the properties of WDM. At present, numerical simulation methods are more popular schemes, such as molecular dynamics (MD) methods¹²⁻¹⁴ and density functional theory¹⁵⁻¹⁷ (DFT). Most of these models are based on the Born-Oppenheimer (BO) approximation. BO approximation—decouples ions from electrons to the instantaneously adjusting potential energy surface (PES) formed by fast electrons—has achieved great success on complex many-body systems. However, it may have difficulty in WDM considering the excitation and ionization of electrons. The drastic dynamic electron-ion collisions cause great disturbances in the PES, and the non-adiabatic effect will exhibit significant effects on the equilibrium and the non-equilibrium processes¹⁸⁻²¹. With the improvement of diagnostic methods, especially the application of X-ray Thomson scattering techniques²², electronic information of WDM can be obtained in the laboratory. To interpret the experimental data, a more precise theory beyond BO approximation is required on account of the complex environment of WDM.

The non-adiabatic effect has been considered by some methods to get more accurate interactions between electrons and ions in WDM. Derived from time-dependent Kohn-Sham

equation, time-dependent density function theory²³ (TDDFT) gives the relatively exact electronic structure information. Thanks to the coupling of the electrons and ions, TDDFT-Ehrenfest approach can give the results such as energy dissipation process, excitation energies and optical properties *etc*^{24,25}. However, TDDFT is extremely time-consuming, limited by finite time and size scale. Thus low frequency modes can not be described well and the convergence of scale is required to be verified carefully. Quantum Langevin molecular dynamics (QLMD) holds a more efficient first principles computation efficiency, simultaneously regarding dynamic electron-ion collisions as frictional forces in Langevin dynamical equation of ions²⁶. Using the QLMD method, a stronger ionic diffusive mode at low frequency has been found when the selected friction parameter becomes larger, as well as the decrease of the sound-speed²⁷. Nevertheless, the determination of the friction parameter is *a priori*. Recently, Simoni *et al* have provided ab-initio calculations of the friction tensor in liquid metals and warm dense plasma²⁸. They obtain a non-diagonal friction tensor, reflecting the anisotropy of instantaneous dynamic electron-ion collisions. Electron force field (EFF) expresses electrons as Gaussian wave packets, so that it can include the non-adiabatic effect intrinsically in molecular dynamics simulation^{29,30}. Lately the method has been applied to warm dense aluminum and found similar conclusions that non-adiabatic effect enhances ion modes around $\omega = 0$, however, the effect is not sensitive to the sound speed³¹. Q. Ma *et al* have developed the EFF methodology to study warm and hot dense hydrogen^{32,33}. They conclude that dynamic electron-ion collisions reduce the electrical conductivities and increase the electron-ion temperature relaxation times compared with adiabatic and classical framing theories. As another approach, Bohmian trajectory formalism has been applied by Larder *et al* recently³⁴. Constructing a thermally averaged, linearized Bohm potential, fast dynamical computation with coupled electronic-ionic system is achieved³⁴. The result also reveals different phenomenon of dynamic structure factor (DSF) and dispersion relation from DFT-MD simulation. All researches reflect that electron-ion collisions affect

^{a)}Electronic mail: jydai@nudt.edu.cn

significantly on the study of dynamic properties of WDM, for both electrons and ions. Nevertheless, the effect of non-adiabatic effect on the ionic transport properties such as diffusion coefficient³⁵ is few studied, in both numerical simulations and analytical models. We could image the existence of dynamic electron-ion collisions will induce new effects such as dissipation or friction. In particular, for the analytical models based on traditional BO methods, we should study the non-adiabatic dynamic collisions effect on the self-diffusion in warm dense matter, and propose a new model including collisions induced friction (CIF).

The paper is organized as follows. Firstly, details of the theoretical methods and the computation of diffusion coefficient are introduced in Section II. Then, in Section III, the static and transport results of QMD, OFMD, QLMD, and (C)EFF simulations are showed and the dynamic collisions effect is discussed. In section IV, we systematically study the collision frequency effect on ionic diffusions and the CIF model is introduced to estimate the impact of electron-ion collisions. In section V, the results are compared with the YOCP, and EOCP models. Finally, the conclusions are given in section VI. All units are in atom unit if not emphasized.

II. THEORETICAL METHODS AND COMPUTATIONAL DETAILS

A. (Constrained) electron force field methodology

EFF method is supposed to be originated from wave packet molecular dynamics (WPMD)³⁶ and floating spherical Gaussian orbital (FSGO) method³⁷. Considering each electronic wave function as a Gaussian wave packet, the excitation of electrons can be included with the evolution of positions and wavepacket radius. N-electrons wave functions are taken as a Hartree product of single-electron Gaussian packet written as

$$\Psi(\mathbf{r}) = \left(\frac{2}{s^2\pi}\right)^{3/4} \exp\left(-\left(\frac{1}{s^2} - \frac{2p_s i}{s\hbar}\right)(\mathbf{r} - \mathbf{x})^2\right) \cdot \exp\left(\frac{i}{\hbar}\mathbf{p}_x \cdot \mathbf{r}\right). \quad (1)$$

where s and \mathbf{x} are the radius and average positions of the electron wave packet, respectively. p_s and \mathbf{p}_x correspond to the conjugate radial and translational momenta. Nuclei in EFF are treated as classical charged particles moving in the mean field formed by electrons and other ions.

Substituting simplified electronic wave function in the time-dependent Schrödinger equation with a harmonic potential, equation of motion for the wave packet can be derived

$$\dot{\mathbf{x}} = \mathbf{p}_x/m_e, \quad (2a)$$

$$\dot{\mathbf{p}}_x = -\nabla_x V, \quad (2b)$$

$$\dot{s} = (4/d)p_s/m_e, \quad (2c)$$

$$\dot{p}_s = -\partial V/\partial s. \quad (2d)$$

where d is the dimensionality of wave packets. For a three-dimensional system, d is equal to 3, and it becomes 2 in 2D systems. V is the effective potential. Combining with ionic equations of motion, EFF MD simulations have been implemented in LAMMPS package³⁰.

In addition to electrostatic interactions and electron kinetic energy, spin-dependent Pauli repulsion potential is added in the Hamiltonian as the anti-symmetry compensation of electronic wave functions. In EFF methodology, the exchange effect is dominated by kinetic energy. All interaction potentials are expressed respectively as

$$E_{nuc-nuc} = \sum_{i<j} Z_i Z_j / R_{ij}, \quad (3a)$$

$$E_{nuc-elec} = \sum_{i<j} -(Z_i / R_{ij}) \operatorname{erf}\left(\sqrt{2}R_{ij}/s_j\right), \quad (3b)$$

$$E_{elec-elec} = \sum_{i<j} (1/r_{ij}) \operatorname{erf}\left(\sqrt{2}r_{ij}/\sqrt{s_i^2 + s_j^2}\right), \quad (3c)$$

$$E_{ke} = \sum_i (3/2) (1/s_i^2), \quad (3d)$$

$$E_{Pauli} = \sum_{\sigma_i=\sigma_i} E(\uparrow\uparrow)_{ij} + \sum_{\sigma_i\neq\sigma_i} E(\uparrow\downarrow)_{ij}. \quad (3e)$$

where Z is the charge of nucleus, r_{ij} and R_{ij} correspond to the relative positions of two particles (nuclei or electrons). $\operatorname{erf}(x)$ is error function, σ means the spin of electrons. Pauli potential is consists of same and opposite spin electrons repulsive potentials. More details can be found in Refs. 29, 30, 38, and 39.

However, the EFF model also suffers from the limitation of WPMD. That is the wave packets spread at high temperature⁴⁰. To avoid excessive spreading of wave packets, the harmonic constraints are often added. Recently, Constrained EFF (CEFF) method has been proposed using $L = \lambda_D + b_0$ as the boundary of the wave packets³², getting much lower electron-ion energy exchange rate agreeing with experimental data^{41,42}.

We use the EFF method to calculate the static and transport properties of hydrogen at $\rho = 5\text{g/cm}^3$ and $\rho = 10\text{g/cm}^3$. The temperature is from 50kK to 300kK. In the simulations, the real electron mass is used so that we choose the time step as small as $0.2as$. 1000 ions and 1000 electrons are used in the simulation. $5ps$ microcanonical ensemble with a fixed energy, volume, and number of particles (NVE) has been performed to calculate statistical average after $10ps$ simulations with fixed temperature, volume, and number of particles (NVT). When the temperature becomes higher, CEFF is applied to avoid wave packets spreading³².

B. Quantum molecular dynamics and orbital-free molecular dynamics

For comparison, we also run the adiabatic simulations including QMD and OFMD. The QMD simulations have been performed using Quantum-Espresso (QE) open-source software⁴³. In QMD simulations, electrons are treated quantum mechanically through the finite temperature DFT (FT-DFT). While ions evolve classically along the PES determined by the electric density, and the electron-ion interaction is described as plane wave pseudopotential. Each electronic wave function is solved by the Kohn-Sham equation⁴⁴

$$\left(-\frac{1}{2}\nabla^2 + V_{\text{KS}}[n_e(\mathbf{r})]\right)\varphi_i(\mathbf{r}) = E_i\varphi_i(\mathbf{r}). \quad (4)$$

where E_i is the eigenenergy, $-1/2\nabla^2$ is the kinetic energy contribution, and the Kohn-Sham potential $V_{\text{KS}}[n_e(\mathbf{r})]$ is given by

$$V_{\text{KS}}[n_e(\mathbf{r})] = v(\mathbf{r}) + \int \frac{n_e(\mathbf{r}')}{|\mathbf{r}-\mathbf{r}'|} d\mathbf{r}' + V_{\text{xc}}[n_e(\mathbf{r})]. \quad (5)$$

where $v(\mathbf{r})$ is the electron-ion interaction, the second term in the right hand of the above equation is the Hartree contribution, an $V_{\text{xc}}[n_e(\mathbf{r})]$ represents the exchange-correlation potential, which is represented by the Perdew-Burke-Ernzerhof (PBE) functional⁴⁵ in the generalized-gradient approximation (GGA) during the simulations. The electronic density consists of single electronic wave function

$$n_e(\mathbf{r}) = 2 \sum_i |\varphi_i(\mathbf{r})|^2. \quad (6)$$

In our simulations, only the Γ point ($\mathbf{k} = 0$) is sampled in the Brillouin-zone, and we used supercells containing 256 H atoms. The velocity Verlet algorithm⁴⁶ is used to update position and velocity of ions. The time step is set from 0.05fs to 0.1fs at different temperature to ensure convergence of energy. The cutoff energy is tested and set from 100 Ry to 150 Ry. The number of bands is sufficient for the occupation of electrons. Each density and temperature point is performed for at least 4000-10000 time steps in the canonical ensemble, and the ensemble information is picked up after the system reaches equilibrium.

At high temperatures, the requirement of too many bands limits the efficiency of QMD method. OFMD is a good choice when dealing with high temperature conditions⁴⁷⁻⁵⁰. Within orbital-free frame, the electronic free energy is expressed as

$$F_e[\mathbf{R}, n_e] = \frac{1}{\beta} \int d\mathbf{r} \left\{ n_e(\mathbf{r}) \Phi[n_e(\mathbf{r})] - \frac{2\sqrt{2}}{3\pi^2\beta^{3/2}} I_{\frac{3}{2}} \{ \Phi[n_e(\mathbf{r})] \} \right\} + \int d\mathbf{r} V_{\text{ext}}(\mathbf{r}) + \frac{1}{2} \iint d\mathbf{r} d\mathbf{r}' \frac{n_e(\mathbf{r}) n_e(\mathbf{r}')}{|\mathbf{r}-\mathbf{r}'|} + F_{\text{xc}}[n_e(\mathbf{r})]. \quad (7)$$

where \mathbf{R} is the ionic position, $\beta = 1/k_B T$ where T is the temperature and k_B is the Boltzmann constant. I_ν is the Fermi integral of order ν . $V_{\text{ext}}(\mathbf{r})$ represents the external or the electron-ion interaction, and $F_{\text{xc}}[n_e(\mathbf{r})]$ is the exchange-correlation potential. The electrostatic screening potential is

represented by $\Phi[n_e(\mathbf{r})]$ depend on electronic density $n_e(\mathbf{r})$ only

$$\nabla^2 \Phi[n_e(\mathbf{r})] = 4\pi n_e(\mathbf{r}) = \frac{4\sqrt{2}}{\pi^2\beta^{3/2}} I_{\frac{1}{2}} \{ \Phi[n_e(\mathbf{r})] \}. \quad (8)$$

The OFMD simulations are performed with our locally modified version of PROFESS⁵¹. The PBE functional⁴⁵ is also used to treat the exchange-correlation potential. 256 H atoms are also used in the supercell. The kinetic energy cutoff is 7000eV when the density $\rho = 5\text{g/cm}^3$, and 10000eV at $\rho = 10\text{g/cm}^3$. The time step is set from 0.04fs to 0.15fs with the temperature increasing. The size effect has been tested in all MD simulations.

C. Quantum Langevin molecular dynamics

QMD and OFMD are good tools in describing static properties of warm dense matters. However, the information of electron-ion dynamical collisions is lost because of the assumption of BO approximation. In addition, electron-ion collisions are important for WDM in which electrons are excited because of the increasing temperature and density. To describe the dynamic process, QMD has been extended by considering the electron-ion collision induced friction (EI-CIF) in Langevin equation, and corresponding to the QLMD model²⁶. In QLMD, ionic trajectory is performed using the Langevin equation⁵².

$$M_I \ddot{\mathbf{R}}_I = \mathbf{F} - \gamma M_I \dot{\mathbf{R}}_I + \mathbf{N}_I. \quad (9)$$

where M_I and \mathbf{R}_I is the mass and position of the ion respectively, \mathbf{F} is the force calculated from DFT simulation, γ means the friction coefficient, and \mathbf{N}_I represents a Gaussian random noise. In QLMD, the force produced by real dynamics of electron-ion collisions can be replaced by the friction on account of less time scale of electronic motions comparing with that of ions. The friction coefficient γ is the key parameter should be determined *a-priori*. Generally, at high temperature such as WDM and HDM regimes, the EI-CIF dominates the friction coefficient, and can be estimated from the Rayleigh model⁵³

$$\gamma = 2\pi \frac{m_e}{M_I} Z^* \left(\frac{4\pi n_i}{3}\right)^{1/3} \sqrt{\frac{k_B T}{m_e}}. \quad (10)$$

where m_e is the electronic mass, Z^* is the average ionization degree. In the paper, we used average atom (AA) model, in which the energy level broadening effect is considered, to estimate the average ionization degree. n_i means the ionic number density. There is another way to assess γ based on the Skupsky model^{54,55}, and in this work, we adopted Rayleigh model only considering the hydrogen we studied has high density and high temperature.

To make sure that the particle velocity satisfies the Boltzmann distribution, the Gaussian random noise \mathbf{N}_I should obey the fluctuation-dissipation theorem⁵⁶

$$\langle \mathbf{N}_I(0) \mathbf{N}_I(t) \rangle = 6\gamma M_I k_B T dt. \quad (11)$$

where dt is the time step in the MD simulation. The angle bracket denotes the ensemble average.

D. Self-diffusion coefficient

In MD simulations, the self-diffusion coefficient is often calculated from the velocity autocorrelation function (VACF) using Green-Kubo formula⁵⁷

$$D = \lim_{t \rightarrow \infty} D(t), \quad (12a)$$

$$D(t) = \frac{1}{3} \int_0^t dt \langle \mathbf{v}_i(t) \cdot \mathbf{v}_i(0) \rangle. \quad (12b)$$

in which $\mathbf{v}_i(t)$ is the center of mass velocity of the i th particle at time t , and the angle bracket represents the ensemble average. Generally, the integral is computed in long enough MD trajectories so that the VACF becomes nearly zero and has less contribution to the integral. All the same species of particles are considered in the average to get faster convergent statistical results.

In practical, it is impossible to get a strict convergent result because the infinite simulation is forbidden. Thus, we usually use a exponential function $\langle \mathbf{v}(t) \cdot \mathbf{v}(0) \rangle = a \exp(-t/\tau)$ to fit the VACF to get the self-diffusion coefficient $D = a \cdot \tau$. Where a and τ are fitting parameters determined by a least-squares fit. τ is corresponds to the decay time. In moderate and strong coupling regimes, a more sophisticated fitting expression is need to be considered⁵⁰. In the exponential function fitting, the statistical error can be estimated by⁵⁸

$$\varepsilon = \sqrt{\frac{2\tau}{NT_{traj}}} \quad (13)$$

where N is the number of particles, T_{traj} is the total time in the MD simulation.

III. RESULTS AND DISCUSSION

A. Static and transport properties

We firstly calculate the radial distribution function (RDF) $g(r)$ of H-H, as shown in Fig. 1. It is shown that the RDFs from OFMD calculations agree well with RDFs of QMD results. Moreover, the RDFs calculated from (C)EFF reflect similar microscopic characteristics with QMD and OFMD results, especially when the temperature is relatively low, where the electron-ion collisions are not so important. For these cases, it is appropriate to show the intrinsic different physics between static and transport properties if the RDFs shown are very close to each other. It should be noticed that the RDFs of (C)EFF model shows a little more gradual than QMD's and OFMD's with the increase of temperature. It is deduced that the non-adiabatic effect plays little role in the static structures of warm dense hydrogen shown here, which is similar to the

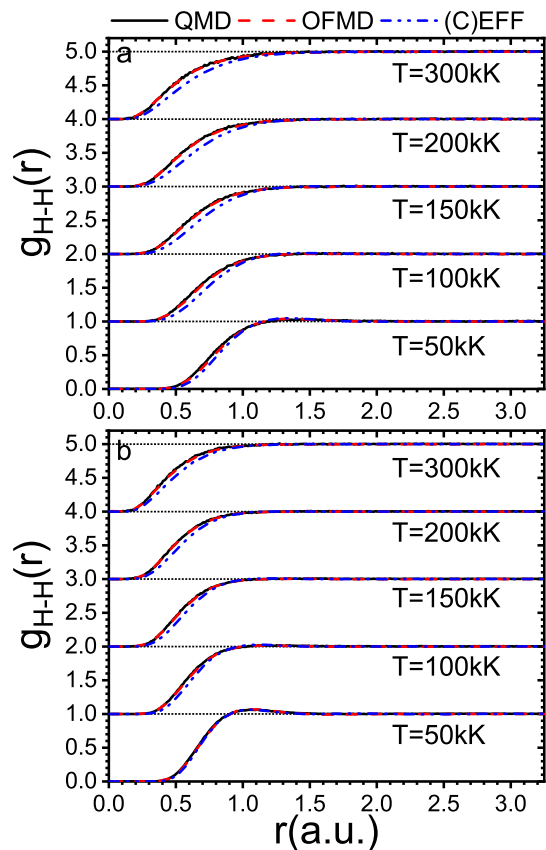


FIG. 1. The RDFs of H-H at 5g/cm^3 (a) and 10g/cm^3 (b). The ordinate is differentiated by adding factors at different temperatures. Blue double dots lines represent the results from (C)EFF simulation. Black solid and red dashed lines are the QMD and OFMD results, respectively.

effects of Langevin dynamics on the static structures^{27,56}, in which the choice of friction coefficients has little effect on the RDFs.

However, non-adiabatic effects on dynamic properties are significant^{26,27,34}. We calculated the self-diffusion coefficients for warm dense hydrogen by integrating the VACF. To get a convergent value, a simple exponential function mentioned in Section II is applied. The self-diffusion coefficient varies with temperature at 5g/cm^3 and 10g/cm^3 are shown in Fig. 2 using different methods of (C)EFF, QMD, and OFMD.

It is very interesting that three methods give consistent results when temperature is relatively low. And the OFMD and QMD results have close values even with the increase of temperature. However, the (C)EFF simulations have a distinct reduce on the self-diffusion coefficients comparing with QMD and OFMD results. And the difference becomes more obvious at higher temperature. We boil it down to the non-adiabatic electron-ion dynamic collisions, which is lost in the framework of BO approximation such as QMD and OFMD. Regarding the electron as a Gaussian wave packet, (C)EFF methodology implements the electron-ion dynamics simulations, in which the dynamic coupling and collisions can be naturally included. As shown in Fig. 2, with the temperature

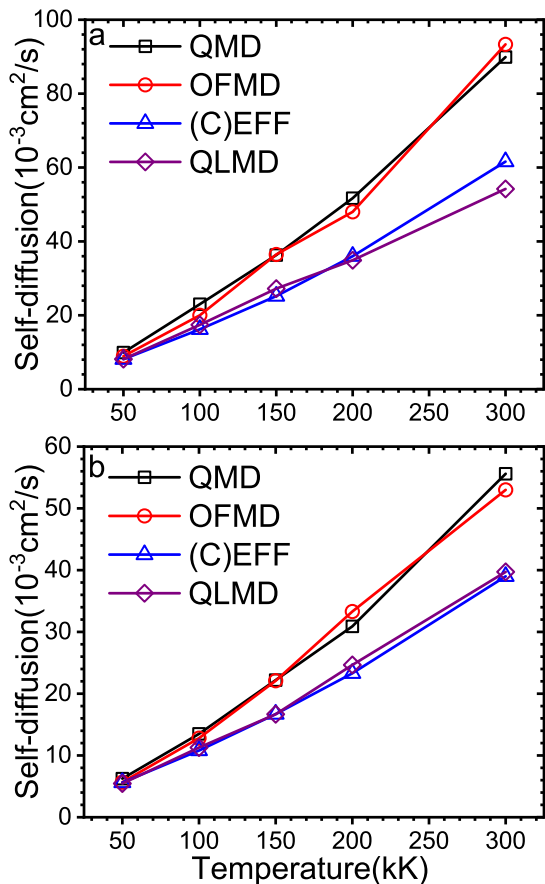


FIG. 2. The self-diffusion coefficients of H as a function of temperature at 5 g/cm^3 (a) and 10 g/cm^3 (b), calculated by QMD, OFMD, QLMD, and (C)EFF methods. Black squares represent the QMD results, red circles are the results of OFMD's, and the (C)EFF results are represented by blue triangles. The QLMD results²⁶ are represented by purple diamonds

increase, more electrons are excited or ionized and become free electrons. These free electrons lead continual and non-negligible electron-ion collisions, supplying drag forces for the motion of ions, and giving rise to much lower diffusion coefficients. The collision rate increases with the temperature, showing lower diffusive properties for ions, significantly affects the transport properties of WDM.

The lost of dynamic collisions can be introduced into the QMD model by considering electron-ion collision induced friction in Langevin equation. Here, we use the Rayleigh model to estimate the friction coefficient γ , and the QLMD simulations have been performed. It is very exciting that the QLMD results, showed in Fig. 2, agree well with (C)EFF simulations. The greatest difference between the two models is 12%, but mostly within 6%. This suggests that the reduction in ionic diffusion from (C)EFF simulations does indeed come from electron-ion dynamic collisions. We believe the small difference belongs to the choice of friction coefficient γ . Since the prior parameter should be determined artificially in QLMD simulations, we are encouraged to do quantitative analysis about the electron-ion collisions effect using

the (C)EFF results as benchmark for the results of all adiabatic methods and analytical models.

IV. ELECTRON-ION COLLISIONS EFFECT ASSESSMENT

As shown above, we should figure out the mechanism how does the dynamic collisions work on the ionic transport? We can find a clue from the Landau-Spitzer (LS) electron-ion relaxation rate (v_{ei})^{59,60}

$$v_{ei} = \frac{8\sqrt{2}\pi n_i Z^2 e^4}{3m_e m_i} \left(\frac{k_B T_e}{m_e} + \frac{k_B T_i}{m_i} \right)^{-3/2} \ln \Lambda \quad (14)$$

where m_e (m_i), n_e (n_i) and T_e (T_i) are the mass, number density and temperature of electrons (ions), respectively. The Coulomb logarithm $\ln \Lambda$ can be calculated by the GMS model⁶¹. In Eq. 14, it is obvious that with the increase of density and temperature (the Coulomb logarithm also varies with the density and temperature), the collision frequency becomes higher, leading the diffusion coefficients reduce more significantly. The results of QMD and (C)EFF simulations showed in Fig. 2 exhibit the same behaviors.

As shown in Eq. 14, the electron-ion relaxation rate (v_{ei}) is the function of temperature and density. However, the thermodynamic state also changes with temperature and density, therefore it is difficult to distinguish the electron-ion collisions effect. For this purpose, we can change the effective mass of electrons in the (C)EFF simulation without altering the intrinsic interactions in the Hamiltonian of the system^{30,62}. Since the mass of ions is much greater than that of electrons, we can find a simple relationship between the electron-ion collision frequency v_{ei} and the mass of the electron m_e from Eq. 14

$$v_{ei} = f(\rho, T) m_e^{1/2} \quad (15)$$

When the dynamic electron mass is larger, the motion of effective electrons exhibit more classical, and the collisions between electrons and ions become stronger. By this way, we can study the influence of electron-ion collisions by adjusting electronic mass in (C)EFF simulations. The VACFs and self-diffusion coefficients of H at different dynamic electron mass are showed in Fig. 3.

From the VACF results we can see, The change of dynamic electron mass does not alter the thermodynamic states of ions. While, dynamic collisions reduce the correlation of particles, showing lower decay time with the increase of dynamic electron mass, as well as the electron-ion collision frequency. Diffusions reflect similar trends, and more interestingly, the diffusion of ions is inversely proportional to the log of electronic mass as showed in Fig. 3(b). The inverse ratio relation reflects the reduction of the diffusion due to electron-ion collisions, and the slope determines the magnitude of this influence. In Fig. 3(b), it is shown that the influence of electron-ion collisions becomes stronger with the increase of temperature, since the electrons are more classical at higher temperature. To quantitatively describe the relationship between diffusion and collision frequency, we performed more intensive simulations on dynamic electron mass as showed in Fig. 4. Here, the

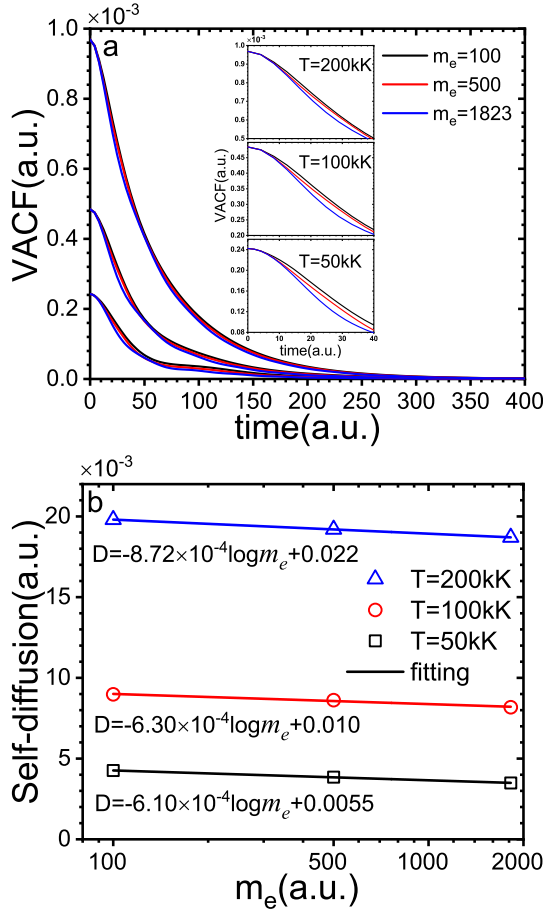


FIG. 3. (a) VACFs of H for different dynamic electron mass at 200kK, 100kK, and 50kK from top to bottom. The density is 10g/cm^3 . The black lines, red lines, and blue lines represent the dynamic electron mass of 100a.u., 500a.u., and 1823a.u., respectively. Details are shown in the insets. (b) The corresponding ionic self-diffusion coefficients as a function of dynamic electron mass. The squares, circles, and triangles represent the temperature at 50kK, 100kK, and 200kK, respectively. The lines are the fitting results, and the fitting functions are listed below the lines.

QMD results are used as the value at reference point, corresponding to no dynamic electron-ion collisions, since m_e can not be zero.

As showed in Fig. 4, the change of diffusion coefficients decreases much steeper when the electron dynamic mass becomes smaller, revealing more significant effect of electron-ion collisions. Another decaying function as $D = a \log(1 + bm_e^c) + d$ can well describe this relation of diffusion varying with the dynamic electron mass m_e . This function can transit to the linear form when m_e is large. Here, we have found the approximate relationship between ionic diffusion coefficient D and electron-ion collision rate v_{ei} taking Eq. 15 into the fitting function

$$D = f_1(\rho, T) \log\left(1 + f_2(\rho, T) v_{ei}^{f_3(\rho, T)}\right) + f_4(\rho, T) \quad (16)$$

where $f_1(\rho, T)$, $f_2(\rho, T)$, $f_3(\rho, T)$, $f_4(\rho, T)$ are the function

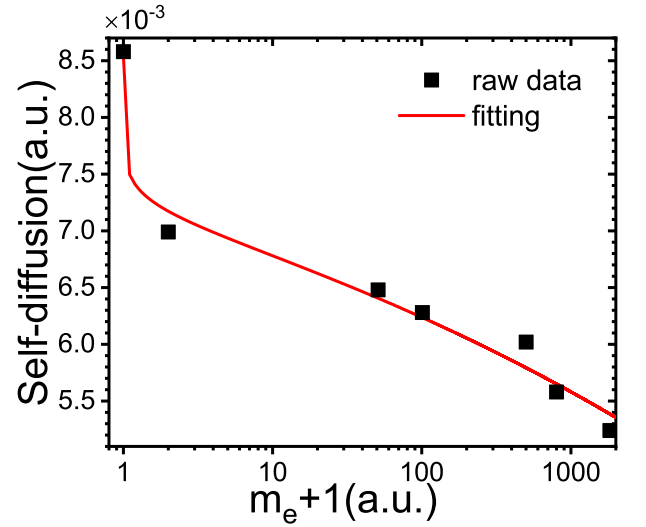


FIG. 4. Dynamic electron mass effects on ionic diffusion. We show the (C)EFF simulation results with different dynamic electron mass at 5g/cm^3 and the temperature is 5kK. The mass of electrons has been shifted to avoid infinity definition of log function at zero point. The value at zero point is replaced by the QMD result. The fitting result is represented by the red line.

of the density ρ and temperature T . If v_{ei} is set to zero, the first term in the right hand of Eq. 16 vanishes, and $D = f_3(\rho, T) = D_0$. Here, the remaining term D_0 represents the diffusion without electron-ion collisions. We call the first term as collisions induced friction (CIF) of the ionic diffusion D_{CIF} . Within this consideration, the total diffusion coefficient can be obtained via

$$D = f_1(\rho, T) \log\left(1 + f_2(\rho, T) v_{ei}^{f_3(\rho, T)}\right) + D_0 \quad (17)$$

$$= D_{\text{CIF}} + D_0$$

For D_0 , plenty of models have been developed to study on it, such as QMD and OFMD which are based on BO approximation. In this paper, the diffusion coefficient including non-adiabatic effect has been calculated using (C)EFF method. As the collision frequency is a small term, the equation can be simplified as $D_{\text{CIF}} = D - D_0 = f(\rho, T) v_{ei}^{f'(\rho, T)}$. D and D_0 can be obtained from (C)EFF and QMD simulations, respectively. We develop an empirical fitting function from the available data as the assessment of electron-ion collisions induced the decrease of ionic diffusions

$$D_{\text{CIF}} = \frac{v_{ei}^{0.25}}{a\rho/T^{3/2} + b\rho + c/T^{3/2} + d} \quad (18)$$

where the fitting coefficient $a = -8.942 \times 10^{-3}$, $b = 1.585 \times 10^{-3}$, $c = 6.849$, and $d = -4.195$. The corrected QMD results by the CIF model, which are shown in Fig. 5, agree well with (C)EFF simulations. To verify the accuracy of the fitting function, we calculate self-diffusion of H and He at some other temperatures and densities. The results are listed in Table I.

In Table I, the ionic self-diffusion coefficients obtained from the QMD model can be modified by adding the CIF fac-

TABLE I. The self-diffusion coefficients calculated by QMD, QLMD and (C)EFF models. The QMD results corrected by the CIF model is also listed in the table.

species	density(g/cm ³)	temperature(K)	$D_{\text{QMD}}(\text{cm}^2/\text{s})$	$D_{\text{QLMD}}(\text{cm}^2/\text{s})$	$D_{\text{(C)EFF}}(\text{cm}^2/\text{s})$	$D_{\text{QMD+CIF}}(\text{cm}^2/\text{s})$
H	8	100000	0.0155	0.0133	0.0122	0.0123
H	8	200000	0.0386	0.029	0.0264	0.0284
H	15	200000	0.0237	0.0181	0.0182	0.0183
H	15	300000	0.0396	0.0289	0.03	0.0278
He	10	100000	0.00757	0.0066	0.00598	0.00596
He	10	200000	0.0181	0.016	0.0108	0.0128

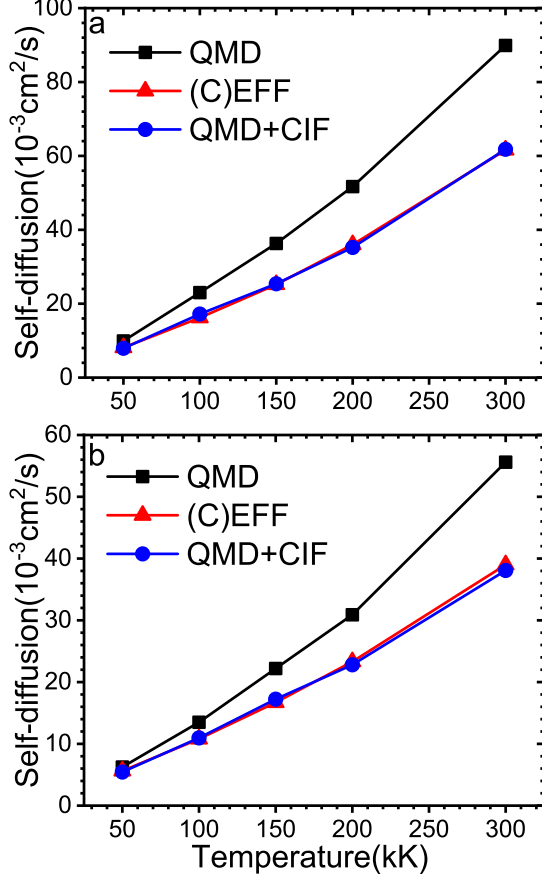


FIG. 5. Self-diffusion coefficients of H calculated by different methods at 5g/cm^3 (a) and 10g/cm^3 (b). The solid black squares and red triangles represent the QMD and (C)EFF results, respectively. The CIF model is used to correct the QMD results as the consideration of non-adiabatic effect. The results are represented by the blue circles.

tor as the compensation of electron-ion collisions. The results are in good agreement with the (C)EFF and QLMD results, showing that our CIF modification can be applied to warm dense matter. It needs to be emphasized that the CIF modification is independent of other models, therefore, any model based on the adiabatic framework can use it to offset the lost of the electron-ion collisions.

V. COMPARISON WITH ANALYTICAL MODELS

The expensive computational costs of first principles simulations make it difficult to apply online or generate large amount of data. On the contrary, some analytical models based on numerical simulations have been proposed, supplying promising approaches to the establishment of database. However, the accuracy of these models should be examined when applied to WDM⁶³. In this section, we use QMD and our modified QMD results as benchmark trying to find an efficient and accurate model to acquire transport parameters.

We firstly compare our results with the Yukawa one-component plasma (YOCP) model, which is a development version of OCP model^{64,65}. In the YOCP model, the electron screening is included to modify the bare Coulomb interactions⁶⁶⁻⁶⁸. The interaction between ions is replaced by the Yukawa potential

$$u(r) = q^2 e^{-\kappa r} / r \quad (19)$$

where κ is the inverse screening length. All properties of the YOCP model are dependent on the inverse screening length κ and the coupling parameter Γ . Daligault has applied the model in a wide range of κ and over the entire fluid region⁶⁹. In the gas-like small coupling regime, the reduced self-diffusion coefficients model can be extended from the Chapman-Spitzer results as⁶⁹

$$D^*(\kappa, \Gamma) = \sqrt{\frac{\pi}{3}} \frac{1}{\alpha(\kappa)} \frac{1}{\Gamma^{5/2} \ln \Lambda(\kappa, \Gamma)} \quad (20)$$

The generalized Coulomb logarithm $\ln \Lambda(\kappa, \Gamma)$ is expressed as

$$\ln \Lambda(\kappa, \Gamma) = \ln \left(1 + B(\kappa) \frac{\lambda_D}{b_c} \right) = \ln \left(1 + \frac{B(\kappa)}{\sqrt{3} \Gamma^{3/2}} \right) \quad (21)$$

where λ_D is the Debye length $\lambda_D = \sqrt{4\pi q^2 n / k_B T}$ and b_c is the classical distance of closest approach $b_c = Zq^2 / k_B T$. $\alpha(\kappa)$ and $B(\kappa)$ are fitting parameters dependent on κ only

$$\alpha(\kappa) = \sqrt{\frac{3}{\pi}} \frac{1}{a_0 + a_1 \kappa^{a_2}} \quad (22)$$

$$B(\kappa) = b_0 + b_1 \text{erf} \left(b_2 \kappa^{b_3} \right) \quad (23)$$

with $a_0 = 1.559773, a_1 = 1.10941, a_2 = 1.36909, b_0 = 2.20689, b_1 = 1.351594, b_2 = 1.57138, \text{ and } b_3 = 3.34187$.

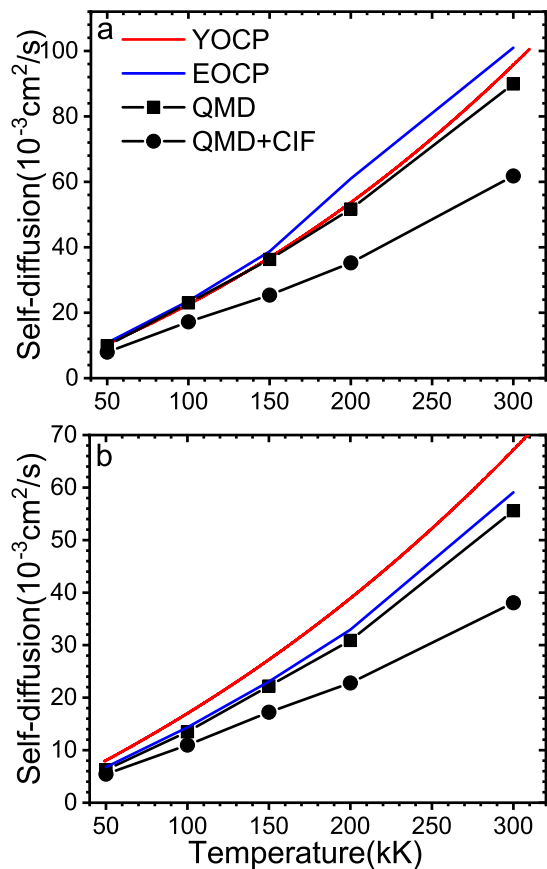


FIG. 6. Comparison of QMD and modified QMD simulations with different analytical models for self-diffusion coefficients of warm dense H at 5 g/cm^3 (a) and 10 g/cm^3 (b). The black solid squares and circles represent the results calculated by QMD and QMD with CIF correction, respectively. The red and blue solid lines are the results of the YOCP model⁶⁹ and EOCP model⁷¹. The effective coupling parameters of the EOCP model are obtained from the RDFs of QMD.

Here, we use the Thomas-Fermi (TF) length²² to estimate the screening of electrons, so that

$$\kappa = \frac{1}{\lambda_{TF}} = \frac{1}{(\pi/12Z)^{1/3} \sqrt{r_i}} \quad (24)$$

where Z is the ionic charge, and r_i is the Wigner-Seitz radius defined as $r_i = (3/(4\pi n_i))^{1/3}$. The self-diffusion coefficient is obtained according to $D = D^* \omega a^2$, and $\omega = (4\pi n_i Z^* e^2 / m_i)^{1/2}$, where Z^* is the average ionization degree which is calculated by the AA model⁷⁰. The comparison between the results of different models are shown in Fig. 6. The QMD results and the CIF modification of QMD's are also shown as benchmarks.

As shown in Fig. 6, for warm dense hydrogen at the density of 5 g/cm^3 , the YOCP model can excellently reproduce results from the QMD simulations. However, at higher density, the YOCP model overestimates the diffusions compared with QMD results. This is because TF length overestimates the screening. With the density increase, electronic charges

are excluded from dense ions that ionic repulsion becomes stronger at short range^{72,73}. And the correlation of ions becomes weaker leading to lower diffusions which is not considered in the TF model. To modify the YOCP model, we should adjust screening length artificially^{74,75}. There is another scheme to deal with larger ionic coupling systems, in which we can reduce effective volumes of particles so that the collision frequency can be increased and the ionic transportation can be dragged or dissipative. The model has successfully improved the transport properties of strongly coupled plasmas in the range $1 \leq \Gamma \leq 30$ ^{73,76,77}.

As another method, the EOCP model has a better description for all density and temperature range we studied with the QMD simulations as shown in Fig. 6. In EOCP model, The effective coupling parameter Γ_e and ionization Q_e are introduced as the correction of the OCP model to reproduced the static structures of the OFMD's⁷⁸, the model also works well on transports properties such as diffusion and viscosity^{71,79}. In this paper, we set Γ_e by the procedure developed by Ott *et al*⁸⁰ as

$$\Gamma_e = 1.238 \exp(1.575 r_{1/2}^3) - 0.931, \quad (r_{1/2} < 1.3) \quad (25)$$

where $r_{1/2}$ is obtained from the RDFs $g(r)$ at $g(r) = 0.5$, The distance is expressed in the Wigner-Seitz radius unit. The effective average charge Q_e is defined as $Q_e = \sqrt{\Gamma_e a k_B T} / e$. We use the RDFs of QMD's as the input of EOCP model, the results agree well with those extracted from long time MD simulations, especially when temperature is low. Compared to the YOCP model, the EOCP model results give a more reasonable description of ionic diffusions. The EOCP model extracts the information directly from the static structure of the system. While the accuracy of the YOCP model depends on the selection of the particle interactions, which should be modeled *a priori*.

However, neither model agrees well with modified QMD results. This can be attributed to the loss of the non-adiabatic effect of the two models. Both the YOCP model and the EOCP model calculate self-diffusion coefficients based on the static potential, and the dynamic electron ion collisions can not be considered in it. This reminds us to pay attention to the instantaneous dynamic collisions effect when doing MD simulations. For application, we can use the CIF model to modify the EOCP model, which is a cheaper way to obtain the self-diffusion data including the non-adiabatic effect.

VI. CONCLUSION

We have performed QMD, OFMD, and (C)EFF simulations to determine the RDFs and the ionic self-diffusion coefficients of warm dense hydrogen at the densities of 5 g/cm^3 and 10 g/cm^3 and temperatures from 50 kK to 300 kK . The results from (C)EFF-MD method are carefully compared with the results from QMD/OFMD methods based on the BO approximation. In EFF method, the static properties are insensitive to electron-ion collisions, however, the diffusion of ions decreases significantly with the increase of electron-ion

collisions. The ionic diffusion coefficients calculated from (C)EFF agree well with the QLMD results, but largely differ from QMD or OFMD simulations, revealing key role of electron-ion collisions in warm dense hydrogen. Most importantly, we proposed a new analytical model which introduce the electron-ion collisions induced friction (CIF) effects, constructing a formula to calculate self-diffusion coefficients without doing non-adiabatic simulations. The CIF model has been verified to be valid over a wider range of temperature, density and materials. However, since the CIF model is derived from the fitting of simulation results, whether it can be applied for more complex elements should be verified further. We also show the results from analytical models of YOCP and EOCP. Based on the static information, EOCP model reproduces QMD simulations better. However, neither of the two models considers the dynamic electron-ion collisions effect. We propose to use the CIF model to modify the EOCP results as a preferred scheme to calculate self-diffusion coefficients.

VII. ACKNOWLEDGMENTS

The authors thank Dr. Zhiguo Li for his helpful discussion. This work was supported by the Science Challenge Project under Grant No. TZ2016001, the National Key R&D Program of China under Grant No. 2017YFA0403200, the National Natural Science Foundation of China under Grant Nos. 11774429 and 11874424, the NSAF under Grant No. U1830206. All calculations were carried out at the Research Center of Supercomputing Application at NUDT.

VIII. DATA AVAILABLE

The data that support the findings of this study are available within the article.

- ¹V. E. Fortov, *Extreme States of Matter: on Earth and in the Cosmos*, 1st ed., The Frontiers Collection (Springer-Verlag Berlin Heidelberg, 2011).
- ²L. G. Stanton and M. S. Murillo, "Ionic transport in high-energy-density matter," *Phys. Rev. E* **93**, 043203 (2016).
- ³A. J. White, L. A. Collins, J. D. Kress, C. Ticknor, J. Cl  rouin, P. Arnault, and N. Desbiens, "Correlation and transport properties for mixtures at constant pressure and temperature," *Phys. Rev. E* **95**, 063202 (2017).
- ⁴R. Heinonen, D. Saumon, J. Daligault, C. Starrett, S. Baalrud, and G. Fontaine, "Diffusion coefficients in the envelopes of white dwarfs," eprint arXiv:2005.05891 (2020).
- ⁵L. A. Collins, V. N. Goncharov, J. D. Kress, R. L. McCrory, and S. Skupsky, "First-principles investigations on ionization and thermal conductivity of polystyrene for inertial confinement fusion applications," *Phys. Plasmas* **23**, 042704 (2016).
- ⁶B. Xu and S. X. Hu, "Effects of electron-ion temperature equilibration on inertial confinement fusion implosions," *Phys. Rev. E* **84**, 016408 (2011).
- ⁷N. Nettelmann, R. Redmer, and D. Blaschke, "Warm dense matter in giant planets and exoplanets," *Phys. Part. Nucl.* **39**, 1122 (2008).
- ⁸B. Xu and S. X. Hu, "Effects of electron-ion temperature equilibration on inertial confinement fusion implosions," *Phys. Rev. E* **84**, 016408 (2011).
- ⁹D. Kang, Y. Hou, Q. Zeng, and J. Dai, "Unified first-principles equations of state of deuterium-tritium mixtures in the global inertial confinement fusion region," *Matter and Radiation at Extremes* **5**, 055401 (2020).
- ¹⁰H. G. Rinderknecht, H. Sio, C. K. Li, A. B. Zylstra, M. J. Rosenberg, P. Amendt, J. Delettrez, C. Bellei, J. A. Frenje, M. Gatu Johnson, F. H. S  guin, R. D. Petrasso, R. Betti, V. Y. Glebov, D. D. Meyerhofer, T. C. Sangster, C. Stoeckl, O. Landen, V. A. Smalyuk, S. Wilks, A. Greenwood, and A. Nikroo, "First observations of nonhydrodynamic mix at the fuel-shell interface in shock-driven inertial confinement implosions," *Phys. Rev. Lett.* **112**, 135001 (2014).
- ¹¹S. Huang, W. Wang, and X. Luo, "Molecular-dynamics simulation of Richtmyer-Meshkov instability on a Li-H₂ interface at extreme compressing conditions," *Phys. Plasmas* **25**, 062705 (2018).
- ¹²J. N. Glosli, F. R. Graziani, R. M. More, M. S. Murillo, F. H. Streitz, M. P. Surh, L. X. Benedict, S. Hau-Riege, A. B. Langdon, and R. A. London, "Molecular dynamics simulations of temperature equilibration in dense hydrogen," *Phys. Rev. E* **78**, 025401 (2008).
- ¹³T. Haxhimali, R. E. Rudd, W. H. Cabot, and F. R. Graziani, "Diffusivity in asymmetric yukawa ionic mixtures in dense plasmas," *Phys. Rev. E* **90**, 023104 (2014).
- ¹⁴Q. Ma, J. Dai, D. Kang, Z. Zhao, J. Yuan, and X. Zhao, "Molecular dynamics simulation of electron-ion temperature relaxation in dense hydrogen: A scheme of truncated coulomb potential," *High Energy Density Phys.* **13**, 34 (2014).
- ¹⁵J. Dai, D. Kang, Z. Zhao, Y. Wu, and J. Yuan, "Dynamic ionic clusters with flowing electron bubbles from warm to hot dense iron along the hugoniot curve," *Phys. Rev. Lett.* **109**, 175701 (2012).
- ¹⁶J. D. Kress, J. S. Cohen, D. A. Horner, F. Lambert, and L. A. Collins, "Viscosity and mutual diffusion of deuterium-tritium mixtures in the warm-dense-matter regime," *Phys. Rev. E* **82**, 036404 (2010).
- ¹⁷D. A. Horner, F. Lambert, J. D. Kress, and L. A. Collins, "Transport properties of lithium hydride from quantum molecular dynamics and orbital-free molecular dynamics," *Phys. Rev. B* **80**, 024305 (2009).
- ¹⁸A. Ng, "Outstanding questions in electron-ion energy relaxation, lattice stability, and dielectric function of warm dense matter," *Int. J. Quantum Chem.* **112**, 150-160 (2012).
- ¹⁹T. S. Strickler, T. K. Langin, P. McQuillen, J. Daligault, and T. C. Kilian, "Experimental measurement of self-diffusion in a strongly coupled plasma," *Phys. Rev. X* **6**, 021021 (2016).
- ²⁰B. Lu, D. Kang, D. Wang, T. Gao, and J. Dai, "Towards the same line of liquid-liquid phase transition of dense hydrogen from various theoretical predictions," *Chin. Phys. Lett.* **36**, 103102 (2019).
- ²¹Q. Zeng and J. Dai, "Structural transition dynamics of the formation of warm dense gold: From an atomic scale view," *SCIENCE CHINA Physics, Mechanics & Astronomy* **63**, 263011 (2020).
- ²²S. H. Glenzer and R. Redmer, "X-ray Thomson scattering in high energy density plasmas," *Rev. Mod. Phys.* **81**, 1625 (2009).
- ²³M. Campetella, F. Maschietto, M. J. Frisch, G. Scalmani, I. Ciofini, and C. Adamo, "Charge transfer excitations in TDDFT: A ghost-hunter index," *J. Comput. Chem.* **38**, 2151 (2017).
- ²⁴F. Graziani, M. P. Desjarlais, R. Redmer, and S. B. Trickey, *Frontiers and Challenges in Warm Dense Matter*, 1st ed., Lecture Notes in Computational Science and Engineering 96 (Springer International Publishing, 2014).
- ²⁵A. D. Baczewski, L. Shulenburger, M. P. Desjarlais, S. B. Hansen, and R. J. Magyar, "X-ray thomson scattering in warm dense matter without the chihara decomposition," *Phys. Rev. Lett.* **116**, 115004 (2016).
- ²⁶J. Dai, Y. Hou, and J. Yuan, "Unified first principles description from warm dense matter to ideal ionized gas plasma: Electron-ion collisions induced friction," *Phys. Rev. Lett.* **104**, 245001 (2010).
- ²⁷P. Mabey, S. Richardson, T. White, L. Fletcher, S. Glenzer, N. Hartley, J. Vorberger, D. Gericke, and G. Gregori, "A strong diffusive ion mode in dense ionized matter predicted by langevin dynamics," *Nat. Commun.* **8**, 14125 (2017).
- ²⁸J. Simoni and J. Daligault, "Nature of non-adiabatic electron-ion forces in liquid metals," e-print arXiv:2007.06747 (2020).
- ²⁹J. T. Su and W. A. Goddard III, "Excited electron dynamics modeling of warm dense matter," *Phys. Rev. Lett.* **99**, 185003 (2007).
- ³⁰A. Jaramillo-Botero, J. Su, A. Qi, and W. A. Goddard III, "Large-scale, long-term nonadiabatic electron molecular dynamics for describing material properties and phenomena in extreme environments," *J. Comput. Chem.* **32**, 497 (2011).
- ³¹R. A. Davis, W. A. Angermeier, R. K. T. Hermsmeier, and T. G. White, "Ion modes in dense ionized plasmas through nonadiabatic molecular dynamics," *Phys. Rev. Research* **2**, 043139 (2020).
- ³²Q. Ma, J. Dai, D. Kang, M. S. Murillo, Y. Hou, Z. Zhao, and J. Yuan, "Extremely low electron-ion temperature relaxation rates in warm

- dense hydrogen: Interplay between quantum electrons and coupled ions," *Phys. Rev. Lett.* **122**, 015001 (2019).
- ³³Q. Ma, D. Kang, Z. Zhao, and J. Dai, "Directly calculated electrical conductivity of hot dense hydrogen from molecular dynamics simulation beyond kubo-greenwood formula," *Phys. Plasmas* **25**, 012707 (2018).
- ³⁴B. Larder, D. O. Gericke, S. Richardson, P. Mabey, T. G. White, and G. Gregori, "Fast nonadiabatic dynamics of many-body quantum systems," *Sci. Adv.* **5**, eaaw1634 (2019).
- ³⁵J. P. Hansen, I. R. McDonald, and E. L. Pollock, "Statistical mechanics of dense ionized matter. III. dynamical properties of the classical one-component plasma," *Phys. Rev. A* **11**, 1025 (1975).
- ³⁶E. J. Heller, "Time-dependent approach to semiclassical dynamics," *J. Chem. Phys.* **62**, 1544 (1975).
- ³⁷A. A. Frost, "Floating spherical gaussian orbital model of molecular structure. i. computational procedure. lih as an example," *J. Chem. Phys.* **47**, 3707–3713 (1967).
- ³⁸J. T. Su and W. A. Goddard III, "The dynamics of highly excited electronic systems: Applications of the electron force field," *J. Chem. Phys.* **131**, 244501 (2009).
- ³⁹P. L. Theofanis, A. Jaramillo-Botero, W. A. I. Goddard, and H. Xiao, "Nonadiabatic study of dynamic electronic effects during brittle fracture of silicon," *Phys. Rev. Lett.* **108**, 045501 (2012).
- ⁴⁰P. E. Grabowski, A. Markmann, I. V. Morozov, I. A. Valuev, C. A. Fichtl, D. F. Richards, V. S. Batista, F. R. Graziani, and M. S. Murillo, "Wave packet spreading and localization in electron-nuclear scattering," *Phys. Rev. E* **87**, 063104 (2013).
- ⁴¹P. Celliers, A. Ng, G. Xu, and A. Forsman, "Thermal equilibration in a shock wave," *Phys. Rev. Lett.* **68**, 2305 (1992).
- ⁴²T. G. White, N. J. Hartley, B. Borm, B. J. B. Crowley, J. W. O. Harris, D. C. Hochhaus, T. Kaempfer, K. Li, P. Neumayer, L. K. Pattison, F. Pfeifer, S. Richardson, A. P. L. Robinson, I. Uschmann, and G. Gregori, "Electron-ion equilibration in ultrafast heated graphite," *Phys. Rev. Lett.* **112**, 145005 (2014).
- ⁴³P. Giannozzi, S. Baroni, N. Bonini, M. Calandra, R. Car, C. Cavazzoni, D. Ceresoli, G. L. Chiarotti, M. Cococcioni, I. Dabo, A. D. Corso, S. de Gironcoli, S. Fabris, G. Fratesi, R. Gebauer, U. Gerstmann, C. Gougousis, A. Kokalj, M. Lazzeri, L. Martin-Samos, N. Marzari, F. Mauri, R. Mazzarello, S. Paolini, A. Pasquarello, L. Paulatto, C. Sbraccia, S. Scandolo, G. Sclauzero, A. P. Seitsonen, A. Smogunov, P. Umari, and R. M. Wentzcovitch, "QUANTUM ESPRESSO: a modular and open-source software project for quantum simulations of materials," *J. Phys. Condens. Matter* **21**, 395502 (2009).
- ⁴⁴R. D. Cowan, *The theory of atomic structure and spectra*, 4th ed., Los Alamos series in basic and applied sciences, 3 (Univ. of California, 2001).
- ⁴⁵J. P. Perdew, K. Burke, and M. Ernzerhof, "Generalized gradient approximation made simple," *Phys. Rev. Lett.* **77**, 3865–3868 (1996).
- ⁴⁶L. Verlet, "Computer "experiments" on classical fluids. I. thermodynamical properties of lennard-jones molecules," *Phys. Rev.* **159**, 98 (1967).
- ⁴⁷Z. Wang, J. Tang, Y. Hou, Q. Chen, X. Chen, J. Dai, X. Meng, Y. Gu, L. Liu, G. Li, Y. Lan, and Z. Li, "Benchmarking the effective one-component plasma model for warm dense neon and krypton within quantum molecular dynamics simulation," *Phys. Rev. E* **101**, 023302 (2020).
- ⁴⁸J. G. Clérouin and S. Bernard, "Dense hydrogen plasma: Comparison between models," *Phys. Rev. E* **56**, 3534 (1997).
- ⁴⁹L. Collins, I. Kwon, J. Kress, N. Troullier, and D. Lynch, "Quantum molecular dynamics simulations of hot, dense hydrogen," *Phys. Rev. E* **52**, 6202 (1995).
- ⁵⁰E. R. Meyer, J. D. Kress, L. A. Collins, and C. Ticknor, "Effect of correlation on viscosity and diffusion in molecular-dynamics simulations," *Phys. Rev. E* **90**, 043101 (2014).
- ⁵¹M. Chen, J. Xia, C. Huang, J. M. Dieterich, L. Hung, I. Shin, and E. A. Carter, "Introducing profess 3.0: An advanced program for orbital-free density functional theory molecular dynamics simulations," *Comput. Phys. Commun.* **190**, 228 – 230 (2015).
- ⁵²D. Kang and J. Dai, "Dynamic electron-ion collisions and nuclear quantum effects in quantum simulation of warm dense matter," *J. Phys. Condens. Matter* **30**, 073002 (2018).
- ⁵³A. V. Plyukhin, "Generalized fokker-planck equation, brownian motion, and ergodicity," *Phys. Rev. E* **77**, 061136 (2008).
- ⁵⁴S. Skupsky, "Energy loss of ions moving through high-density matter," *Phys. Rev. A* **16**, 727 (1977).
- ⁵⁵L. G. Stanton, J. N. Glosli, and M. S. Murillo, "Multiscale molecular dynamics model for heterogeneous charged systems," *Phys. Rev. X* **8**, 021044 (2018).
- ⁵⁶J. Dai and J. Yuan, "Large-scale efficient langevin dynamics, and why it works," *Europhys. Lett.* **88**, 20001 (2009).
- ⁵⁷R. Kubo, "Statistical-mechanical theory of irreversible processes. I. general theory and simple applications to magnetic and conduction problems," *J. Phys. Soc. Japan* **12**, 570 (1957).
- ⁵⁸B. Hess, "Determining the shear viscosity of model liquids from molecular dynamics simulations," *J. Chem. Phys.* **116**, 209 (2002).
- ⁵⁹L. D. Landau, "The transport equation in the case of coulomb interactions," *Zh. Eksp. Teor. Fiz.* **7**, 203 (1937), [*Phys. Z. Sowjetunion* **10**, 154 (1936)].
- ⁶⁰L. Spitzer, *Physics of Fully Ionized Gases* (Interscience, New York, 1967).
- ⁶¹D. O. Gericke, M. S. Murillo, and M. Schlages, "Dense plasma temperature equilibration in the binary collision approximation," *Phys. Rev. E* **65**, 036418 (2002).
- ⁶²P. L. Theofanis, A. Jaramillo-Botero, W. A. Goddard, T. R. Mattsson, and A. P. Thompson, "Electron dynamics of shocked polyethylene crystal," *Phys. Rev. B* **85**, 094109 (2012).
- ⁶³Z. Li, Y. Cheng, Q. Chen, and X. Chen, "Equation of state and transport properties of warm dense helium via quantum molecular dynamics simulations," *Phys. Plasmas* **23**, 052701 (2016).
- ⁶⁴J. Daligault, "Liquid-state properties of a one-component plasma," *Phys. Rev. Lett.* **96**, 065003 (2006).
- ⁶⁵J. Daligault, "Erratum: Liquid-state properties of a one-component plasma [phys. rev. lett. 96, 065003 (2006)]," *Phys. Rev. Lett.* **103**, 029901 (2009).
- ⁶⁶S. Hamaguchi, R. T. Farouki, and D. H. E. Dubin, "Triple point of yukawa systems," *Phys. Rev. E* **56**, 4671 (1997).
- ⁶⁷M. S. Murillo, "Viscosity estimates for strongly coupled yukawa systems," *Phys. Rev. E* **62**, 4115 (2000).
- ⁶⁸J. Daligault, "Diffusion in ionic mixtures across coupling regimes," *Phys. Rev. Lett.* **108**, 225004 (2012).
- ⁶⁹J. Daligault, "Practical model for the self-diffusion coefficient in yukawa one-component plasmas," *Phys. Rev. E* **86**, 047401 (2012).
- ⁷⁰Y. Hou, F. Jin, and J. Yuan, "Influence of the electronic energy level broadening on the ionization of atoms in hot and dense plasmas: An average atom model demonstration," *Phys. Plasmas* **13**, 093301 (2006).
- ⁷¹J. Clérouin, P. Arnault, C. Ticknor, J. D. Kress, and L. A. Collins, "Unified concept of effective one component plasma for hot dense plasmas," *Phys. Rev. Lett.* **116**, 115003 (2016).
- ⁷²H. Sun, D. Kang, Y. Hou, and J. Dai, "Transport properties of warm and hot dense iron from orbital free and corrected yukawa potential molecular dynamics," *Matter Radiat. Extremes* **2**, 287 (2017).
- ⁷³J. Daligault, S. D. Baalrud, C. E. Starrett, D. Saumon, and T. Sjostrom, "Ionic transport coefficients of dense plasmas without molecular dynamics," *Phys. Rev. Lett.* **116**, 075002 (2016).
- ⁷⁴G. Zérah, J. Clérouin, and E. L. Pollock, "Thomas-fermi molecular-dynamics, linear screening, and mean-field theories of plasmas," *Phys. Rev. Lett.* **69**, 446 (1992).
- ⁷⁵J. Clérouin and J.-F. Dufreche, "Ab initio study of deuterium in the dissociating regime: Sound speed and transport properties," *Phys. Rev. E* **64**, 066406 (2001).
- ⁷⁶S. D. Baalrud and J. Daligault, "Modified enskog kinetic theory for strongly coupled plasmas," *Phys. Rev. E* **91**, 063107 (2015).
- ⁷⁷S. D. Baalrud and J. Daligault, "Effective potential theory for transport coefficients across coupling regimes," *Phys. Rev. Lett.* **110**, 235001 (2013).
- ⁷⁸J. Clérouin, G. Robert, P. Arnault, J. D. Kress, and L. A. Collins, "Behavior of the coupling parameter under isochoric heating in a high-z plasma," *Phys. Rev. E* **87**, 061101 (2013).
- ⁷⁹P. Arnault, "Modeling viscosity and diffusion of plasma for pure elements and multicomponent mixtures from weakly to strongly coupled regimes," *High Energy Density Phys.* **9**, 711 (2013).
- ⁸⁰T. Ott, M. Bonitz, L. G. Stanton, and M. S. Murillo, "Coupling strength in coulomb and yukawa one-component plasmas," *Phys. Plasmas* **21**, 113704 (2014).